

## Reply to Reviewer 1:

### Reviewer Comments:

This manuscript describes particulate measurements taken along the coast of Southern California. Much of the discussion focuses on the comparison between the AMS and an FTIR-based method, and the two techniques complement each other nicely.

The authors estimate the contribution of SOA to the total OA observed at the sampling site. I believe that their estimates of the fraction of SOA are too low; this conclusion comes at the detriment of the manuscript. The authors estimate that the OA is about 10-30% SOA. However, it seems that the fraction of SOA may be much higher – at least 30-60%. This dominance of SOA is likely the most important conclusion of the manuscript, as the same SOA fraction is determined by both the AMS and FTIR analyses. The FTIR analysis therefore verifies the large fractions of SOA (measured as OOA) observed at numerous sites in the northern hemisphere with AMS's.

Overall, the manuscript is poorly written and organized, and at times is difficult to follow. The interesting technical aspects and scientific conclusions are largely obscured by the poor quality of the writing. The underlying data and analysis will be worthy of publication once the writing is improved.

### Response (blue sections below)

We thank the reviewer for the constructive comments and questions, which have not changed the substance of our study but have greatly helped us to improve the manuscript quality. We have clarified the vague terms (e.g. alkanes) to make sure the terminology is consistent throughout the text. We have re-organized and improved the writing, as outlined below. We have taken special care to clarify a misunderstanding that the Reviewer had that the total SOA was estimated to be 15-30%, when in fact this was only “Today’s SOA”, as described below, and the correct number for Total SOA was 60%, exactly within the range suggested by the Reviewer. We do take exception to the statement that this work in any way “verifies” measurements made in other seasons at other locations, as we have no reason to expect that the fraction of SOA is invariant worldwide, especially since some areas “in the northern hemisphere” are dominated by fossil-fuel combustion emissions and others by biogenic SOA. To illustrate this variability, we have added Table 4 (shown below) to explicitly compare to other SOA fractions found worldwide. While many of these SOA fractions are consistent, we do not assert that is verification but rather similarity.

We calculate the SOA mass using three methods. The first method is based on the assumption that components with high O/C (including carboxylic acid groups and combustion factors in this study) are secondary, and the SOA derived from this calculation is the total SOA (60% of the OM). The second method, and the novel aspect of the SOA calculated in this manuscript, is the SOA formed during the 12-h period of one specific day (which is defined as “Today’s SOA”), i.e. the addition of OM during the daytime, which is only a fraction of the total SOA and lower than the total SOA. The third

method is using the size distribution of oxygenated components to identify how the SOA is formed in the particle phase.

In the revised manuscript, we have clearly distinguished the three methods of SOA calculation in section 4.1, 4.2, and 4.3. We have defined the newly formed SOA during a single day as “Today’s SOA” and referred to the rest of the SOA to “Background SOA,” meaning that it existed before “Today’s SOA” was formed. We have also noted that the total SOA is the sum of these two quantities, and we have included this fraction in the abstract as well to make this clear.

The revised abstract reflecting these changes now reads:

“Carboxylic acids are present in substantial quantities in atmospheric particles, and they play an important role in the physical and chemical properties of aerosol particles. During measurements in coastal California in the summer of 2009, carboxylic acid functional groups were exclusively associated with a fossil fuel combustion factor derived from factor analysis of Fourier transform infrared spectroscopic measurements. The high fraction of acid groups and the high ratio of oxygen to carbon in this factor suggest that this factor is composed of secondary organic aerosol (SOA) products of combustion emissions from the upwind industrial region (the ports of Los Angeles and Long Beach). Another indication of the photochemically-driven secondary formation of this combustion-emitted organic mass (OM) was the daytime increase in the concentrations of acid groups and the combustion factor. This daytime increase closely tracked the O<sub>3</sub> mixing ratio with a correlation coefficient of 0.7, indicating O<sub>3</sub> was closely associated with the SOA maximum and thus likely the oxidant that resulted in acid group formation. Using a pseudo-Lagrangian framework to interpret this daytime increase of carboxylic acid groups, we estimate that carboxylic acid groups formed as “Today’s SOA” contribute 10% of the measured OM, while the remaining carboxylic acid groups (25% of the OM) were likely formed 1-3 days previously (the “Background SOA”). A similar estimate of the daytime increase in the combustion factor suggests that “Today’s SOA” contributed to 15–30% of the OM, and the “Background SOA” accounted for 30–45% of the OM, for a total SOA contribution to OM of 45-75%. Further, size-resolved spectrometric and spectroscopic characterizations of the particle organics indicate that the majority of the OM formed by condensation of gas-phase oxidation products. This unique set of approaches for quantifying and characterizing photochemically and ozone-linked carboxylic acid group formation provide independent and consistent assessments of the secondary fraction of OM, which could result from second generation products of the oxidation of gas-phase alkane (molecules).”

To improve the writing and organization of the manuscript, we have taken the following steps:

1. We have revised the discussion in section 4 to clearly outline our method for identifying SOA in the context of AMS and other prior results; we have discussed the “chemical-composition” based SOA in section 4.1; then we have introduced the pseudo-Lagrangian approach to using diurnal patterns to evaluate “Today’s

SOA” in section 4.2; we have revised the discussion of (m/z 44)/nrOM and nrOM/PM<sub>AMS</sub> size distributions in section 4.3 (see below); and we have compared explicitly the SOA identified using the three methods in section 4.4.

2. We have simplified the description of the two types of carboxylic acid group profiles in section 3.3. The revised paragraph is shown in the answers to the “Specific questions” below.
3. We have clarified the SOA terminology and calculation in sections 4.1, 4.2, and 4.3 (see below).
4. We have moved the detailed discussion of “PMF factors” to the appendix, so that more detail can be added on the method for selecting factors without distracting from the acid-focus of the manuscript.
5. Transition sentences are added to the introduction to make it easier to follow.
6. The figures are now corrected so that they are cited in order; in addition, we have moved the figure captions so that their display in ACPD format is more easily readable (especially Figures 3, 6, and 12).

#### Specific questions:

\*Page 7191 – The discussion of the importance of “alkane groups” to ambient OA is confusing. I interpret the FTIR-determined alkane groups to indicate aliphatic carbons—those with only C-C and C-H bonds. However, starting in line 26, the authors convolve “alkane groups” with “alkanes” (e.g., Lim and Ziemann, Presto et al). The authors should either be more explicit in their definition of alkane groups or consider using a different term, such as aliphatic groups.

We have used “alkane groups” throughout the text to specify that we measured alkane functional groups in the particle phase rather than the molecule. We prefer this terminology to the more chemically-specific terminology of “aliphatic, saturated groups” as it is more widely used (and shorter) and consequently more understandable to a broader audience (and it avoids the creation of yet another acronym – ASG or SAG). In contrast, we have used “gas-phase alkane (molecules)” to refer to the gas-phase precursors that lead to the formation for carboxylic acid groups. We have also defined the functional groups at the beginning of the text:

Page 1190, Line 25-26, change “The major organic components identified in ambient particles include alkane, carboxylic acid, hydroxyl, amine, and non-acid carbonyl functional groups” to “The major organic components identified in ambient particles include alkane (saturated C-C-H), carboxylic acid (C(O)OH), hydroxyl (C-OH), amine (C-NH), and non-acid carbonyl (C=O) functional groups”.

\*Page 7195 – The first figure referenced in the text is Fig. 3, followed by Figs. 1 and 5. The figures should be referenced in order.

The figure order has been corrected in the revised manuscript.

\*Page 7196 and Figure 3a – Lines 20-22 of page 7196 note “Only days associated with single air mass sector (32 out of 47 days) were included (Fig. 3a) in the diurnal cycle analysis in order to track the daily changes in composition caused by chemistry rather than air mixing,” and the caption to Figure 3a says “top green bars indicate samples associated with single air mass sector, which were used for diurnal profile analysis.” I think that the authors are trying to say that the days labeled with the green bar in Figure 3a were days where the sampling site was impacted by air from a single air mass sector, and that there were 32 such days in the 47 days of the study. However, the green bars in Figure 3a clearly cross days represented by different air masses, and in some cases a single day is indicated as being influenced by more than one source region (e.g., August 20-21, August 30-September 1). The explanation both in the text and the figure caption require clarification.

We apologize; we had a bug in the code that generates the top bars, which caused the unmatched gaps of the green bars and the “air mass indicator” bars and we failed to catch this when we proofread the submission. We have corrected this in the revised manuscript (see below “list of revised figures”). Also, the “single day” in this study is defined as “6 am - 6 am”, which is also clarified on Page 7196, line 20.

\*Page 7197, Section 3.3 – It is not clear why the authors determined the background CO mixing ratio with a plot of OM vs CO, especially considering that the background CO mixing ratio differed for the FTIR and AMS analyses. Why not use the CO measured during time periods when the sampling site was impacted by the “Ocean” trajectory in Figure 1 as the background CO? Also, it is not clear that the differences in the intercepts for the FTIR and AMS-determined background CO (80 vs 89 ppb) are insignificant, because the authors do not note average or extreme concentrations of CO measured at the sampling site.

The “background CO” can be defined and calculated in several ways. One definition is the CO concentration in the cleanest air mass measured. We did not use this because we are concerned that the “Ocean” air mass in this study could include some background of ship emissions (Dominguez et al., 2008), therefore the CO concentration in the “Ocean” air mass is the polluted CO rather than background CO. The method used in this study is based on the concept proposed by DeCarlo et al. (2010) that the “background CO” is the CO concentration associated with nearly zero OM, which we obtain by extrapolation of the CO to where OM=0. This approach does ignore primary biogenic contributions to OM such as marine aerosol from breaking waves (Russell et al., 2010), but for this study that difference was likely small (Hawkins and Russell, 2010, *Atm. Env.*, although it may contribute to the difference between FTIR and AMS).

We applied both the FTIR OM and the AMS nrOM versus CO to get a robust “background CO”. Since the difference between AMS- and FTIR- determined CO (9 ppb) is small compared to the ambient variations ( $\pm 71$  ppb), we used the average of the AMS- and FTIR- determined CO as the “background CO” for consistency for both the AMS and the FTIR measurements throughout the study.

We have revised the text to clarify that we are using the same “background CO” for both the FTIR and the AMS measurements. We have also reported the average and standard deviation of the CO concentration:

Add to Page 7197, line 22: replace “Since the difference of the two intercepts is insignificant (10%), an average value of 85 ppb was used as the background CO mixing ratio.” with “Since the difference of the two intercepts is small relative to the ambient variations (which had a standard deviation of 71 ppb), an average value of 85 ppb was used as the background CO mixing ratio for both the FTIR and the AMS measurements.”

\*Page 7198, Line 19 – This is the first reference to Figure 2, and it comes after references to Figures 1, 3, 4, 5, and 6. As a reader I find the disjointed numbering of the figures thoroughly confusing. Also, there is such little discussion of Figure 2 that I am not sure it warrants a place in the manuscript.

We apologize for the error. As noted above, we have re-ordered the figures to match the citation order in the revised manuscript.

We have moved Figure 2 to the appendix because we agree it is not essential to the main argument of the manuscript but it is important to explain the variations of carboxylic acid group concentrations in nighttime samples. In addition, we have also revised Figure 1 (see “list of revised figures” below) to better show both the trajectories and the wind directions during the campaign.

\*Page 7198, Line 1 to Page 7199, Line 5 – The discussion of the classification of the diurnal profiles is difficult to follow, with four “Types” and two “Classes.” The text seems to describe the thought process that was used to parse the sampling days into types and classes, which may be too much detail. It would be much simpler to state that the days are classified as either “Afternoon high” or “Noon high”, and to describe the minor differences within each class of days.

These two paragraphs have been simplified according to the suggestion. Fig. 6 is revised to better describe the types of the diurnal patterns (see “list of revised figures” below). The revised paragraph reads:

“Diurnal profiles of normalized carboxylic acid group concentrations are classified into the “Afternoon High” and the “Noon High” types (Fig. 4). Both types show higher concentrations at local noon (solar maximum) relative to the early morning period, while they differ in whether the concentration peaked at noon or after noon: the “Afternoon High” type days (type A) have peak concentrations in the afternoon and “Noon High” type days (type B) have peak concentrations at noon. For days within each type, nighttime carboxylic acid group concentrations were variable, with concentrations that were sometimes higher and other times lower than the noon and afternoon values. The variability in concentration at night is likely the result of variations in the land-sea breeze circulations, as illustrated in Fig. B1. Winds coming from the northwest dominate during daytime and easterlies dominate at night. The variability in nighttime concentrations

within each type likely resulted from different air masses brought by the nighttime easterlies. In contrast, there was no evidence for impacts on daytime concentrations from variable sea breezes during the day, consistent with the nearly constant northerly winds shown in Fig. B1 for all days selected for this study. For this reason, our analysis has focused only on the daytime measurements, when the constant wind direction provided a consistent source and nearly constant transport times for emissions from the ports of Los Angeles and Long Beach, making the time series measurements effectively pseudo-Lagrangian.”

\*Page 7199, Line 6 – I am not familiar with “Aged Combustion Factor,” and I don’t think that the average reader will be either. While the Aged Combustion Factor is described nicely in the subsequent PMF section, it is used both here and in the Abstract with no explanation. This makes the paper difficult to read, and in fact I did not understand large sections of the manuscript until my second reading because, frankly, it is out of order. The PMF classes should be introduced earlier, or not used at all until they are discussed. The description of Figure 7 on page 7199 would not suffer if the authors only discussed the AMS m/z 44.

We thank the Reviewer for this suggestion. We did refer to section 3.4.2 for the “Aged Combustion Factor” to provide more details on this usage, but to avoid this problem the PMF section has been moved to the appendix and briefly introduced before the diurnal cycle section (3.3) in the revised version. The figures in these two sections are re-ordered accordingly. In the abstract, the “Combustion factor” is introduced prior to the discussion as well (see revised abstract text above).

\*Page 7199, Line 23 – Page 7200, Line 11 – I do not think that the discussion of Figure 9 adds significantly to the manuscript. It should either be expanded or removed.

The STXM-NEXAFS measurement provides an opportunity to investigate the photochemical processing of the particles from a single particle perspective. This measurement is complementary to the FTIR and AMS measurements. We have expanded the discussion of the STXM-NEXAFS measurements, including the calculation of the carboxylic acid group mass fractions, and compared explicitly to the other measurements.

Page 7196, Line 16: add to the end of the first paragraph: “The OM mass fraction of carboxylic acid groups in single particles, calculated as carboxylic acid group absorption normalized by the sum of absorption of all functional groups from the X-ray spectra, are  $42\pm 14\%$  for the morning particles and  $38\pm 17\%$  for the afternoon. These values are comparable to the carboxylic acid group fraction of 34% from the submicron FTIR measurement, given the uncertainties and approximations in both methods. There was no measurable difference in the number or mass fraction of carboxylic acid groups in the afternoon particles compared to the morning particles (likely due to the small number of particles (37 in total) that could be analyzed with the limited beamtime available), but the results support the presence of carboxylic acid groups in submicron particles, as expected for SOA formation (Claeys et al., 2007). Further, it is worth noting that acid

groups are prevalent throughout the particles, rather than being limited to surface coatings.”

\*Page 7201, Lines 5-10 – The authors should give more explanation to why they combined the 6 factors from the PMF solution into three. As they note in line 5, the three-factor solution is not sufficient to describe the variability in the data. How is collapsing the 6-factor solution into three factors better? I assume that the three combined factors were used to facilitate comparison with the 3-factor AMS solution, but perhaps this hides some information from the FTIR PMF solution? I assume that 6 factors were needed to describe the data because there is additional information in the FTIR spectra that is not available in the AMS.

We agree that we should provide more information on the selection of FTIR and AMS PMF factors. For this reason, we have moved this discussion to Appendix A, where it has been expanded without interfering with the main focus of the article (as per the concern of the Short Comment). The appendix describing PMF analysis now reads:

## “Appendix A

### A1 PMF of the FTIR spectra

PMF was applied to the 234 mass-weighted and baselined FTIR spectra. The scaling factors were estimated by baselining errors calculated using the automated algorithm described by Russell et al. (2009a). The robust mode was used and the outliers were downweighted during the fitting procedure. Two to six factors with an FPEAK range of [0,  $\pm 0.2$ ,  $\pm 0.4$ ,  $\pm 0.6$ ,  $\pm 0.8$ ,  $\pm 1$ ] were tested. Plotting Q (the sum of squared scaled residuals) versus FPEAK showed that the lowest Q values corresponded to FPEAK of -0.2, 0, and 0.2, which resulted in the same factors. The edge-FPEAK values [ $\pm 0.6$ ,  $\pm 0.4$ ,  $\pm 0.8$ , and  $\pm 1$ ] resulted in increased Q values, indicating increased residuals associated with the PMF model (Lanz et al., 2007). Because the sensitivity to rotation was negligible for FPEAK=-0.2, 0, and 0.2, FPEAK=0 was selected to represent the solution.

Q can also be used as a mathematical diagnostic of the PMF solutions.  $Q/Q_{\text{exp}}$  (normalized Q), in which  $Q_{\text{exp}}$  approximately represents the degree of freedom of the fitted data, is greater than 4 for the two- and three-factor solutions and smaller than 3 for the  $n>3$  solutions (Fig. A1). This decrease of normalized Q indicates that the additional factors in the  $n>3$  solutions explain significantly more variation of the data. Therefore, two- and three-factor solutions were excluded.

Factors that correlated ( $r>0.5$ ) with similar compositions were identified in the four-, five-, and six- factor solutions, indicating some factors that split into indistinguishable and non-independent components (Ulbrich et al., 2009). The correlated factors in each solution were combined to one factor, resulting in three factors for each of the four-, five-, and six-factor solutions. The combined factors explain the same degree of the OM variability as the individual factors used from the four-, five-, and six-factor solutions, and the combined factor mass is equal to the sum of individual factor masses. The three recombined factors resulting from the six-factor solution were selected

because these factors captured events that were associated with trajectories from either known wildfires or from Los Angeles-Long Beach ports. In addition, the factor profiles had similar peak structure ( $r > 0.8$ ) with the known factors derived from the TEXAQS/GoMACCS 2006 and the Scripps Pier 2008 measurements (Hawkins and Russell, 2010a; Russell et al., 2009a).

The factors were identified by comparing factor spectrum and composition with previously identified factors. The first factor spectrum correlated to the fossil fuel combustion factor profiles of the TEXAQS/GoMACCS (Russell et al., 2009a) and the Scripps Pier 2008 measurements (Hawkins and Russell, 2010a) projects with  $r$  of 0.97 and 0.99, respectively, indicating similar organic compositions from similar sources or processes. This factor was characterized by large fractions and co-existence of alkane and carboxylic acid functional groups (51% and 42% of the factor OM, respectively) and was identified as a fossil fuel combustion factor. The concentration of this factor was  $3.0 \mu\text{g m}^{-3}$ , accounting for 62% of the OM on average (Fig. 2c). Hydroxyl and amine functional groups contributed 7% and 1% of the factor OM, respectively. The PSCF image (Fig. A2a) shows the origin of this factor was mainly located at the vicinity of the Los Angeles region, which are dominated by fossil fuel combustion emissions. The second factor spectrum correlated to the biomass burning factor profiles identified from the TEXAQS/GoMACCS (Russell et al., 2009a) and the Scripps Pier 2008 measurements (Hawkins and Russell, 2010a) with  $r$  of 0.87 and 0.93, respectively. The factor fraction time series (Fig. 2c) showed three high concentration periods: 26 August–2 September, 8–22 August, and 22–27 September, corresponding to the three largest fires (by acreage) that occurred in the Southern California region that summer: the Station fire (in Los Angeles County), the La Brea fire (in Santa Barbara County), and the Guiberson fire (in Ventura County), respectively (<http://www.fire.ca.gov/fire-protection/fire-protection-fire-info-redbooks-2009.php>). The PSCF image (Fig. A2b) indicates that this factor is likely from north of Los Angeles – Santa Barbara County, as well as Baja California regions, consistent with fire events that occurred during the sampling period and fire maps from satellite measurements (Fig. A2c). Based on the similarity of this factor spectrum to previously identified biomass burning factors and the increase in concentration during fire-influenced time periods, this factor was identified as a biomass burning factor. The factor concentration was  $0.88 \mu\text{g m}^{-3}$  on average and accounted for 18% of the OM. Non-acid carbonyl and alkane functional groups dominated this factor, accounting for 44% and 34% of the factor OM, respectively. The factor spectrum of the third factor was comparable ( $r=0.82$ ) to the spectrum of the polluted marine factor described in the Scripps Pier 2008 measurements (Hawkins and Russell, 2010a). This factor was identified as a marine factor that accounted for 20% of the OM on average and was dominated by hydroxyl functional groups (72%). Alkane, carboxylic acid, and amine functional groups contributed 20%, 4%, and 3% of the OM, respectively. The concentration and composition of the factors are summarized in Table 2.

## A2 PMF of organic fragment concentrations

PMF was applied to the time series of concentrations of 271 AMS-measured organic mass fragments. The input matrix and the error files for PMF of the AMS measurements were prepared using the Igor Pro 5 (Wavemetrics Inc.) codes based on

the work of Zhang et al. (2005). Two to six factors with FPEAK-range of [0,  $\pm 0.2$ ,  $\pm 0.4$ ,  $\pm 0.6$ ,  $\pm 0.8$ ,  $\pm 1$ ] were investigated. The Q versus FPEAK plot shows the lowest Q values corresponding to FPEAK values of -0.2, 0, and 0.2. The factors generated for each rotation were nearly indistinguishable. FPEAK=0 was selected to represent the solutions. A distinct factor with significant mass was missing when two factors were used. For each of the four-, five-, and six-factor solutions, highly correlated factors ( $r > 0.7$ ) were combined, resulting in three recombined factors, which resembled the three factors generated from the three-factor solution. The normalized Q values for the three-six factor solutions are comparable (differences are within 10%), indicating three factors were enough for explaining the variability of the input data matrix. Therefore, the three-factor solution was selected, which reproduced 98% of the OM.

The factors were identified by comparing normalized factor spectra with the online AMS reference spectra (Ulbrich et al., 2007, 2009). The first factor  $m/z$  spectrum correlated to several LVOOA (low-volatility OOA) and SOA spectra. For example, the factor spectrum correlated to the Pittsburgh OOA factor spectrum (Zhang et al., 2005;  $r = 0.93$  for  $m/z > 44$  and  $r = 0.95$  for all  $m/z$ ) and the spectrum from the photooxidation of *m*-xylene with seed aerosols under RH=55% (Bahreini et al., 2005;  $r = 0.94$  for  $m/z > 44$  and  $r = 0.90$  for all  $m/z$ ). The factor could not be further split into LV-OOA and SV-OOA (semi-volatile OOA) factors as shown in many previous studies (Ng et al., 2010), likely because of the relatively low particle concentration at the sampling site as well as the lower resolution of the quadrupole MS. The diurnal cycle of this factor showed a significant increase in concentration during the day and lower values in the morning and at night (Fig. 5), indicating photochemical origins of this factor. This factor likely represented an aged component formed from processed primary emissions. The factor was identified as an aged combustion factor, which accounted for 61% of the  $nrOM_{AMS}$  and was associated with the largest  $m/z$  44  $nrOM$  fraction and the largest  $m/z$  44 to  $m/z$  43 ratio of all of the factors (Table 2). The second factor profile strongly correlated with the wood burning spectrum ( $r = 0.90$  for both  $m/z > 44$  for all  $m/z$ ) identified by Lanz et al. (2007) and the brush fire spectrum ( $r = 0.94$  for  $m/z > 44$  and  $r = 0.92$  for all  $m/z$ ) described by Bahreini et al. (2005). This factor was identified as a biomass burning factor, accounting for 26% of the  $nrOM$ . No correlation was found between the third factor spectrum and the spectra from the AMS database. The factor concentration correlated to none of the concentrations of the AMS-measured inorganic compounds. The factor profile correlated moderately ( $r = 0.5$ ) with the third factor (which was likely influenced by the ocean) from the ICEALOT study (Frossard et al., 2011) and the time series correlated to that of the FTIR marine factor with  $r = 0.5$ . This factor may be a shipping or marine factor, which accounted for 13% of the  $nrOM$ .”

\*Section 4.1 -I am not convinced that the strong correlation between carboxylic acid groups and ozone is the smoking gun that the authors suggest. Ozone tends to be highly correlated with OH, and one could consider the periods of high ozone as periods of high photochemical activity, with abundant OH available to participate chemistry.

We agree that OH radicals co-exist with  $O_3$  during daytime and that they participate in the formation of carboxylic acid groups. However, the interesting thing about this data set is that there is an observed offset between solar maximum (and inferred OH

concentration) and SOA maximum. Further, OH oxidation alone does not produce SOA with carboxylic acid groups (Lim and Ziemann 2005; 2009). We hypothesize that the alkane group reaction is initiated by abstraction of an H atom by OH radical, forming an alkyl radical. The alkyl radical undergoes isomerization, cyclization, and dehydration processes, forming dihydrofuran (Page 7206, line 9), which evaporates and primarily reacts with O<sub>3</sub> (Russell et al, 2011) to form carboxylic acid groups. While carboxylic acid groups correlate to O<sub>3</sub>, no correlation is found between carboxylic acid groups and photosynthetically active radiation (PAR; Fig. 1 in this document), which represents the solar radiation and can be used as an indicator for OH radicals. This again suggests the O<sub>3</sub>-driven formation of carboxylic acid groups. We have added “DHF primarily with O<sub>3</sub> (Russell et al., 2011; Martin et al., 2002)” on Page 7206, line 11 to address the unique role of O<sub>3</sub> in the formation of carboxylic acid groups.

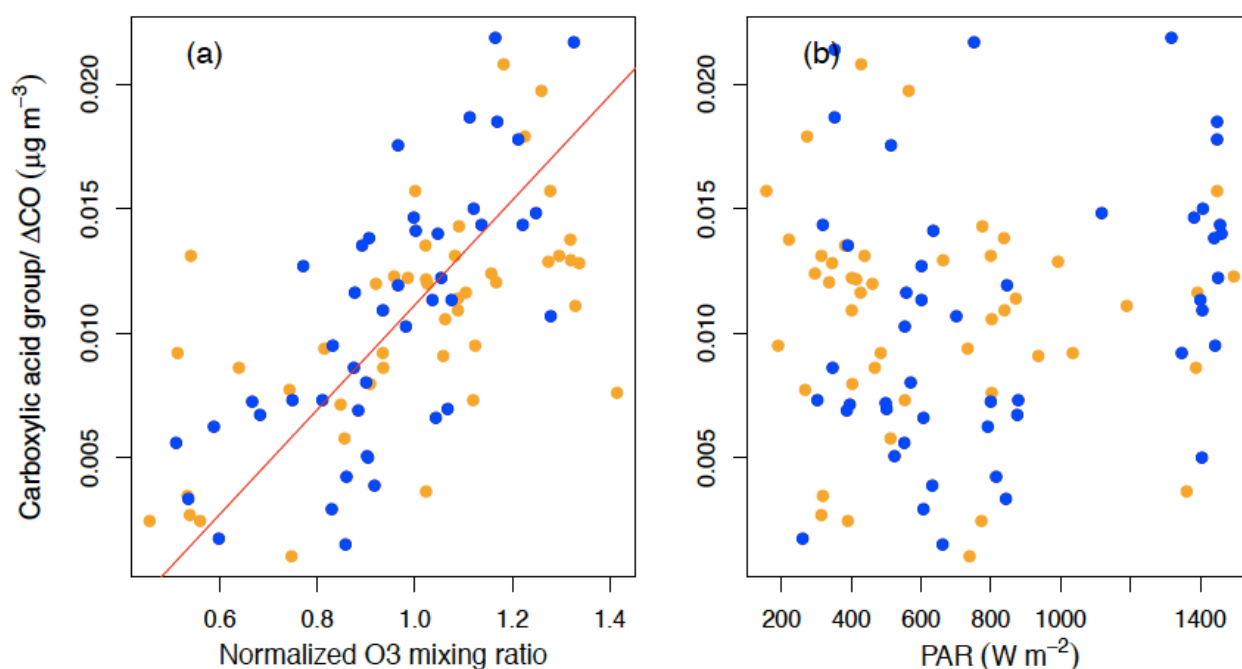


Fig. 1 Correlation of normalized carboxylic acid group concentration and (a) normalized O<sub>3</sub> mixing ratio (by campaign average) and (b) PAR for the “Afternoon High” (orange) and “Noon High” (blue) type of days.

In the last paragraph on page 7205, which continues to page 7206, the authors state that acid groups are formed from ozone reactions with dihydrofurans (which are produced by isomerization and dehydration in the particle phase). However in the following paragraph, starting on Line 18 of page 7206, the authors further argue that high concentrations of AMS m/z 44 result from condensed phase oxidation. Since AMS m/z 44 is correlated with the FTIR-determined acid groups, aren't these two paragraphs at odds? The first suggests that acids (and therefore AMS m/z 44) form via (1) vapor phase oxidation with OH, (2) condensed phase processing without oxidation, and (3) vapor-phase oxidation by ozone. All of the oxidation in this scheme occurs in the vapor phase.

The second paragraph suggests that AMS m/z 44 (and therefore organic acid groups) form in the condensed phase.

We thank the reviewer for pointing out this apparent contradiction in the results, which was reflected in our initial interpretation. We have re-considered the interpretation of Fig. 11, in light of the conclusion noted that the OM is largely SOA: the similarity of size distributions of m/z 44 and OM and the size-independence of (m/z44)/OM suggest m/z 44 is internally mixed with OM; the decrease in the ratio of nrOM to PM<sub>1</sub> with D<sub>p</sub> indicates a surface-driven process (such as condensation from the gas phase), consistent with our interpretation of the formation of acids in the gas phase from oxidation of dihydrofurans by ozone. The size dependence of (m/z 44)/OM and nrOM/PM<sub>1</sub> indicates that particle-phase OM and m/z 44 (and likely carboxylic acid groups) are formed by condensation of organic vapors, similar to the “Condensation and Surface-limited Oxidation” model of SOA formation (from vapor or particle phase) proposed by Maria et al. (2004), although in that work there was significant preexisting POA in particles, while in this study POA played a small role.

The revised discussion of this topic from Page 7206 is now section 4.3 (shown in the answers to the next question below).

\*Section 4.2 – The calculations used to estimate the SOA mass fraction are unclear, but it seems like the authors are severely underestimating the SOA mass fraction. There are several pieces of evidence to consider: (1) The discussion of the PMF factors notes that the AMS Combustion factor is similar to Pittsburgh OOA, which is often considered as a surrogate for ambient SOA. The fraction of m/z 44 in the AMS Combustion factor is 26%, and the fraction of m/z 57 (tracer for fresh emissions) is negligible. One could easily assume that the Combustion factors are pure SOA. (2) The combustion factors for the AMS and FTIR are the dominant component of the OA at about 60% of the total mass on average. (3) The average contribution of organic acid groups is 34%. This is likely the lower bound estimate for the SOA mass fraction. As noted in Section 4.1, the organic acids are likely secondary in nature.

Figure 12 seems to suggest that the authors assume that the overnight/background OA is primary. I would argue that this is all or at least mostly aged SOA. Changing the grey portions of the bars in Fig 12 to green would significantly increase the SOA mass fraction.

Based on a rough estimate given the items above, it seems that on average the OA is at least between 34-62% SOA. The real value is likely higher, as the biomass burning factor is aged during transit to the sampling site, and is therefore not purely primary OA.

We fully agree that a large fraction of the OM is likely SOA as indicated from the combustion factor and carboxylic acid group mass fractions. We are not sure why the Reviewer interpreted the overnight/background OA in Fig. 12 as primary, unless it is simply because it was grey, which may be used in some AMS papers to mean primary? Either way, we used grey to mean background SOA, namely that SOA formed on the

previous day(s). To prevent such unfortunate misinterpretation in the future, we have changed the color to a different shade of green instead of grey.

Moreover, since it seems that it was not clear to the Reviewer how (or why) we were interested in quantifying not just total SOA (from oxygenated fraction) but “Today’s SOA” (from the amount of SOA added in a single afternoon), we have reorganized section 4 to better explain this in the context of a number of previous studies. In addition, in the revised version, we have repeated and clarified this point and clearly distinguished the “Background SOA” and “Today’s SOA”. A new table (Table 4) is added to help distinguish and compare the methods used for SOA identification and the differing assumptions employed.

We have also further clarified the motivation for estimating how much SOA is formed each day. We have expanded this discussion in the new section 4.4 to make the comparisons of the two methods explicit, i.e. to show that we are forming 15-30% of OM per day, so that the total SOA represents 15-30% of “Today’s SOA” and 30-45% of “Background SOA”.

The new section 4, 4.1, 4.2, 4.3, 4.4 and Table 4 are given below:

#### 4 Discussion

In this section, we identify the fraction of the measured organic mass that is secondary. We start with the approach that is implicit in a number of recent studies (summarized in Table 4), namely that oxygen-containing organic components that are from fossil fuel combustion emissions, and the other (non-oxygen-containing) organic components that co-occur with them, are secondary. Special attention is given to carboxylic acid functional groups, as they are the canonical low-volatility products of photochemical oxidation of hydrocarbons (Haagen-Smit, 1952). Next, we use the assumption of a Lagrangian evolution of the air mass and the availability of daytime sunlight to separate the OM that is produced in a single day of photochemical reactions. Accounting for the expected multi-day lifetime of SOA, we then compare the two different approaches to quantifying SOA. Finally, we note that marine and terrestrial primary biogenic oxygen-containing organic components need to be excluded from both of these estimates, which is possible using PMF separation and tracers for marine production.

##### 4.1 SOA identification by chemical composition: Contributions of acid groups and oxygenated organic fragments

Several studies of tropospheric carboxylic acids (Table 4) proposed that carboxylic acids are formed in the atmosphere, based on observed correlations of carboxylic acids to solar radiation or ozone mixing ratio. These methods of SOA identification are supported by model predictions and smog chamber studies that predicted or measured the formation of carboxylic acids (Madronich et al., 1990; Grosjean et al., 1992, Yu et al., 1999). Although direct emission of carboxylic acids (molecules) was also associated with vehicular exhaust (Kawamura and Kaplan, 1987)

and meat cooking (Rogge et al., 1991), the lack of correlation of carboxylic acids with tracers from these emissions suggests that the contributions from these primary sources are minor. In addition to carboxylic acid groups, other oxygenated groups (e.g. hydroxyl groups and non-acid carbonyl groups) were identified in smog chamber studies (Kleindienst et al., 2004; Sax et al., 2005; Lim and Ziemann, 2005). The common conclusion in these studies is that for most urban sources, the oxygenated fraction of OM is secondary. Using this assumption (that fairly oxygenated OM is SOA), these recent studies in a variety of urban and rural regions have found that 50-100% of the OM measured was SOA (Table 4).

Similarly, if we take this approach to identifying SOA in the Scripps pier measurements (which were dominated by urban emissions from Los Angeles), we find that the fossil fuel combustion factor is likely secondary, given its high fraction of carboxylic acid groups and associated high O/C. This result gives an average “Total SOA” for this study of 60% of the OM, well within the range of these other measurements. Since we have specifically separated out the 40% of OM from non-urban sources (biomass burning and marine OM), it is not surprising that we are at the low end of the 50 to 100% range given in Table 4 (since the studies that reported higher SOA fractions had low non-urban contributions to OM). Furthermore, we can look specifically at what fraction of the SOA is actually acid groups: the “Total SOA” estimated from carboxylic acid groups was 34% of OM, namely half of the SOA (by mass) is carboxylic acid groups.

#### 4.2 SOA identification by pseudo-Lagrangian observations: Daytime formation of carboxylic acid groups and oxygenated organic fragments.

An alternative way to estimate SOA mass fraction is to assess the amount of additional OM formed during the sunny part of a single day. This approach requires measurements in a pseudo-Lagrangian framework, where we can infer that the photochemical exposure (aging) of the emissions tracks with the time of day. In this case, the majority of the volatile organic compounds (VOCs), in particular those from fossil fuel combustion, was emitted in the Los Angeles – Long Beach region. Further, the transit from that emission point to the Scripps Pier was largely over clean marine regions with small OM sources (as in Hawkins and Russell, 2010, *Atm. Env.*). The other aspect of this study region is that northwesterly flow predominated in daytime, thus also providing sufficient regional homogeneity on the selected days, as illustrated by the day-to-day similarities in Figs. 4 and 5.

With this pseudo-Lagrangian approach, we can identify SOA more specifically using the dependence on sunlight and oxidants during a single day, separating SOA into “Background SOA” (formed on prior days) and “Today’s SOA” (formed during a 12-h daytime period of one particular day). In this calculation, “Today’s SOA” contributions from carboxylic acid groups and the combustion factors are both estimated by assuming that the minimum concentration that occurs in the early morning is representative of a background value (the “Background SOA” from formation on previous days) and that the increase that occurs (relative to  $\Delta\text{CO}$ ) is from photochemical processing during one specific 12-h daytime. Since only the combustion factor is accounted for in this

calculation, this method estimates only the portion of “Today’s SOA” from fossil fuel combustion.

To evaluate the time scale of carboxylic acid group formation, we evaluate the lag time between the peak concentrations in  $O_3$  and either  $m/z$  44 or the AMS combustion factor. The peak concentrations of  $m/z$  44 and the AMS combustion factor occurred approximately 1-2 hours later than the  $O_3$  peak for both the “Afternoon High” and the “Noon High” type days (Fig. 5), suggesting that the time scale for the formation of  $m/z$  44 and the AMS combustion factor is 1–2 hours. The good correlations of carboxylic acid groups to  $m/z$  44 and the AMS combustion factor throughout this study allow one to infer that carboxylic acid group formation also had a time scale of 1-2 hr (although a direct observation of the lag is not possible, given the 4-hour duration of the FTIR daytime samples).

#### 4.3 SOA identification by size dependence: Surface-limited condensation of oxygenated organic fragments

The size dependence of the organic components provides additional evidence of how the SOA formed. Representative size distributions of  $m/z$  44 and the AMS nrOM are shown in Fig. 9 for the “Afternoon High” days (for time period of 14:00–18:00) and the “Noon High” days (for time period of 10:00–14:00). For both cases,  $m/z$  44 and nrOM showed similar size distributions with peaks at 300–500 nm, indicating the two components were internally mixed in the particle phase, consistent with the results of the FTIR PMF which associated acid and alkane groups in the combustion factor. The  $m/z$  44 fraction of OM was nearly independent of particle size, while  $nrOM/nrPM_{AMS}$  decreased with increasing particle diameter, consistent with theoretical models in which acid and alkane groups are added proportionally so give a constant ratio with size (Fig. 9-iii) and the total amount of OM increases relative to the particle mass giving a  $1/D_p$  dependence (Fig. 9-iv). This result differs slightly from the model presented by Maria et al. (2004), in which the proportionality of added acid and alkane groups is masked by pre-existing distributions of POA carbon. In this study, the degree and consistency of oxygenation of the fossil fuel combustion fraction (noted in section 4.1) indicates that there was likely no substantial preexisting POA.

Single particle analysis using STXM-NEXAFS provides additional information on the size dependence of SOA formation, including specific identification of carboxylic acid groups. The resulting size dependence of OM/PM decreases with increasing size, similar to Fig. 9-iv, but the small number of particles analyzed (37) is insufficient to justify more than a linear fit (with  $r=-0.6$ ). Interestingly, the size dependence of the acid group fraction of OM increased with increasing size, indicating a possible difference from the  $m/z$  44/OM results (such as non-acid contributions to  $m/z$  44). However, the variability in the acid fraction for the five different sampling days that were included in these 37 analyzed particles was greater than the variability with size, suggesting that the aggregation of five samples (each 15-30 min duration) may not be appropriate. Since we also did not have sufficient AMS signal to obtain a size distribution in 30 min of sampling, it is not possible to rule out other factors.

#### 4.4 Comparison of the three methods of identifying SOA

The three SOA identification methods were employed independently to characterize SOA, so it is worth assessing the extent to which the resulting characterizations are consistent. The “chemical composition” method was used to quantify the SOA mass and fraction based on the oxygenated nature of the organic associated with fossil fuel combustion tracers (summarized in Table 4). The pseudo-Lagrangian method was used to identify the daytime formation of “Today’s SOA” (Table 3 and 4). The “size-dependence” method was used to identify how SOA was formed in the particle phase.

Comparing the two quantitative approaches to SOA, we find from the “chemical composition” method that 60% of OM is SOA. From the “pseudo-Lagrangian” method, we find that 15-30% of OM is “Today’s SOA.” Combining these two results, we find that 25-50% of SOA is formed each day (on average). This finding is consistent with the expected boundary layer lifetime of particles of 4-5 days, suggesting that the submicron SOA remains on average 4 days (more after accounting for losses).

There are two previous studies that have separated recent SOA from background SOA (Table 4). The “Background SOA” fraction used here is analogous to the “Background OA” estimated by Liggio et al. (2010) from measurements at Egbert, Ontario (Table 4), except that rather than looking only at “Today’s SOA” Liggio et al. (2010) evaluated the SOA formed within 24–48 hours. Their estimate for that central Canadian region was 42-71% of the Total SOA (40–50% of the total OM), which is about two times higher than the “Today’s SOA” fraction of 25-50% of the Total SOA (15-30% of the total OM) estimated from the combustion factors found for the coastal region in this study. Given that their time period for “recent” formation was twice as long (and that different sites have different mixtures of sources), the estimates are well within the expected consistency.

We can also look specifically at the acid fraction formed today, which here was found to be 25-33% of the total acid group concentration. Satsumabayashi et al. (1990) found that in central Japan “Today’s acid (molecule) fraction” was 72–84% of the “Total acids (molecules).” However, the pseudo-Lagrangian approach used in Satsumabayashi et al. (1990) was limited to measurements of only two commonly-observed acids, i.e. succinic acid and phthalic acid, and the emissions in central Japan are quite high.

Taking the results of all three approaches together, the co-variation of daytime concentrations and the correlation of overall concentrations ( $r = 0.7$ ) of carboxylic acid groups and  $O_3$  (Fig.4; Fig.8) provides substantial evidence for an  $O_3$ -driven oxidation that forms carboxylic acid groups. The carboxylic acid, hydroxyl, non-acid carbonyl, and alkane group mole fractions of the combustion factor were 0.11, 0.04, 0.00, and 0.85, comparable to the  $C_{12}$  alkane (molecule) oxidation products with mole fractions of 0.12, 0.13, 0.02, and 0.73 estimated by Russell et al. (2011). In the mechanism proposed by Russell et al. (2011), gas-phase alkanes (molecules) are oxidized by OH radicals to form dihydrofuran in the particle phase by H-atom subtraction, isomerization, cyclization, and dehydration processes. Dihydrofuran then evaporates into the gas phase and reacts

primarily with O<sub>3</sub>, producing products that are expected to be similar to cyclic alkene oxidation products, namely multi-functional products with carboxylic acid functional groups (which would be expected to partition into the particle phase due to their low vapor pressures). This mechanism is consistent with the observed SOA composition (for the combustion factor) in this study and the co-variation of carboxylic acid and alkane groups. Combining this information with the size dependence of oxygenated mass fragments (m/z 44) supports the hypothesis that these two functional groups were likely formed in the same molecules in the gas phase and condensed simultaneously on particles as second-generation products of gas-phase alkane (molecule) oxidation.

I think that the most important conclusion from this manuscript is that the FTIR measurements echo the large body of AMS measurements that suggest that SOA is the dominant form of OA in the atmosphere. The authors should state this clearly.

We certainly agree that SOA is the majority of OM for this study, and we believe the revised abstract and section 4 and added tables make this clear. A generalization that “SOA is the dominant form of OA in the atmosphere” from the results presented in this study would be unjustified, but our results at this site are certainly consistent with that generalization.

\*Table 3 – The values in Table 3 are not clear to me. What is different between the numbers in and out of parenthesis?

We have remade the table and specifically labeled the values (see below “revised tables”). The mass concentration of the SOA is added to the table as well to clarify the difference between “Today’s SOA” and “Total SOA”. We have also added a discussion of the fraction of “Total SOA” that is formed each day as “Today’s SOA.”

Comments on Figures \*Figure 3 is too small and therefore hard to read. I had to zoom in significantly to read the details. \*Figure 6 is almost impossible to interpret. I think that the green and blue points represent duplicates of the same days, just plotted on different axes for clarity. This is not obvious from the way the axes are labeled – in fact, it looks like there are sets of organic acid measurements for one day, followed by alkane measurements for the next day. The caption mentions “thick” and “thin” rectangles, but it is not obvious that the rectangles have different line thicknesses. \*I don’t think that Figure 13 adds to the manuscript, and it could be removed.

We have made the figures bigger by moving the caption text to the end of the main text.

Figure 6 is revised (see “list of revised figures”): the diurnal cycles of carboxylic acid and alkane groups are stacked and only the two major types (“Afternoon High” and “Noon High”) are shown. Arrows are added to indicate the peaks. The rectangles of the averages are removed because they largely overlap with the rectangles of individual days. The averages are indicated by the thick lines.

We agree that Figure 13 does not add significantly to the manuscript and it has been removed.

Revised tables:

**Table 3.** Mass concentration and OM fraction of total SOA (estimated from the “chemical-composition” based method) and “Today’s SOA” (estimated from the “pseudo-Lagrangian” based method) calculated from carboxylic acid groups, the FTIR combustion factor, and the AMS combustion factor for the “Afternoon High” and the “Noon High” days.

“Afternoon High” Days

	Concentration ( $\mu\text{g m}^{-3}$ )		Fraction of total OM	
	Total SOA	Today’s SOA	Total SOA	Today’s SOA
Carboxylic Acid Group	1.2	0.3	36%	9%
FTIR Combustion Factor	2.9	1.0	60%	20%
AMS Combustion Factor	2.5	1.1	61%	27%

“Noon High” Days

	Concentration ( $\mu\text{g m}^{-3}$ )		Fraction of total OM	
	Total SOA	Today’s SOA	Total SOA	Today’s SOA
Carboxylic Acid Group	1.0	0.3	30%	10%
FTIR Combustion Factor	3.0	0.7	62%	14%
AMS Combustion Factor	2.1	0.8	51%	19%

**Table 4.** Comparison of SOA mass fractions in this study with previous studies. Quantities include 1) OM fraction of “Total SOA”, 2) OM fraction of “Recent SOA” (SOA formed within 1 day or 2 days), 3) OM fraction of “Background SOA”, 4) OM fraction of carboxylic acid (groups), and 5) ratio of “Recent SOA” to “Total SOA”.

Reference	Total SOA	Recent SOA	Background SOA	Carboxylic Acid (Groups)	Ratio of Recent SOA to Total SOA	Identification of SOA
Schuetzle et al., 1975	–	–	–	–	–	correlation of acids with solar radiation
Cronn et al., 1977	–	–	–	–	–	correlation of acids with solar radiation
Rogge et al., 1993	–	–	–	–	–	correlation of acids with solar radiation
Kawamura and Yasui, 2005	–	–	–	–	–	correlation of acids with solar radiation
Satsumabayashi et al., 1989	–	–	–	–	–	correlation of acids with ozone
Kawamura and Ikushima, 1993	–	–	–	–	–	correlation of acids with ozone
Satsumabayashi et al., 1990 <sup>1</sup>	30–50%	22–42%	58–78%	30–50%	72–84%	correlation of acids with ozone
Hildebrandt et al., 2010	nearly 100%	–	–	–	–	high O/C component
Zhang et al., 2007b	64–95%	–	–	–	–	high O/C component
Lanz et al., 2007	60–69%	–	–	–	–	high O/C component
Gilardoni et al., 2007	50%	–	–	31%	–	high O/C component
Russell et al., 2009a	70%	–	–	31%	–	high O/C component
Liggo et al., 2010	75–95%	40–50%	35–45%	–	42–71%	high O/C component and photochemical age
This study	60%	15–30%	30–45%	34%	25–50%	high O/C component and correlation of acid groups with ozone

<sup>1</sup> SOA fractions were calculated using acid molecules only.

List of revised figures:

Change of figure orders in the revised manuscript:

Figure in the original manuscript	Figure in the revised manuscript
Figure 1	Figure 1
Figure 2	Figure B1
Figure 3	Figure 2
Figure 4	Figure 3
Figure 5	Figure A2
Figure 6	Figure 4
Figure 7	Figure 5
Figure 8	Figure 6
Figure 9	Figure 7
Figure 10	Figure 8
Figure 11	Figure 9
Figure 12	Figure 10
Figure 13	Removed

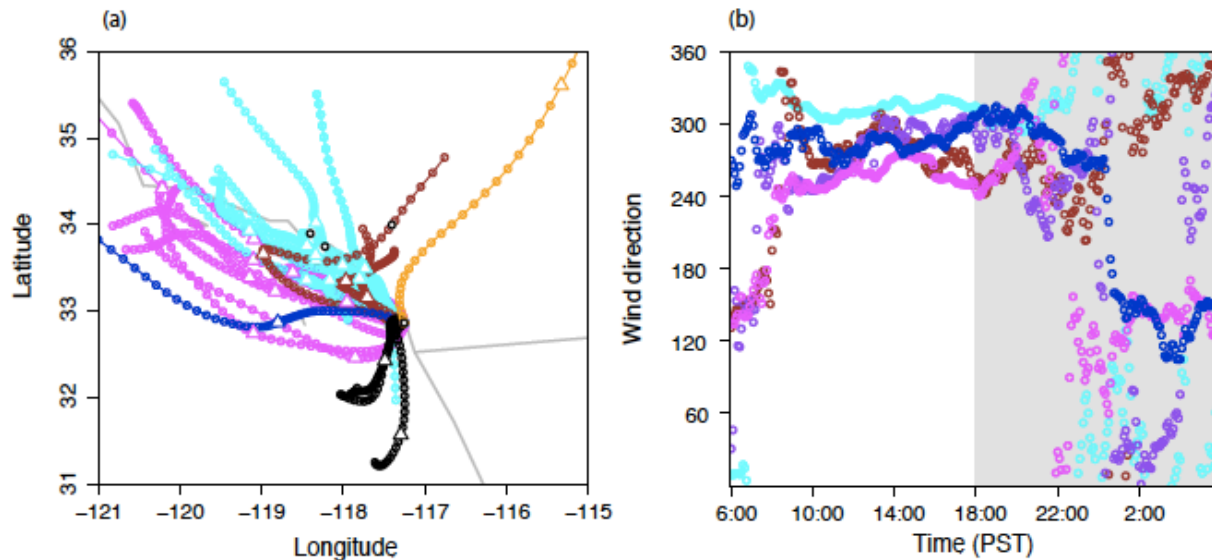


Fig. 1. (a): Averaged 48-h back trajectories for each day (daytime only) representing Los Angeles-Long Beach (cyan; air mass coming from Los Angeles and Long Beach regions), Riverside (brown; air mass originating from Riverside vicinity), Inland (orange; easterly/northeasterly air mass), Tijuana-Ensenada (black; southerly air mass), Mixed coastal (magenta; northerly air mass coming along the coast of California), and Ocean (dark blue; westerly air mass) air mass sectors during the campaign. The triangle in each trajectory indicates 48-h before the air mass arrived at the sampling site. The black circles (from top to bottom) indicate Riverside, Los Angeles, Los Angeles - Long Beach port, and the sampling site; (b) vector-averaged diurnal profile of wind direction (0 degree represents wind coming from north) for the air mass sectors specified in (a). Shaded areas indicate nighttime periods.

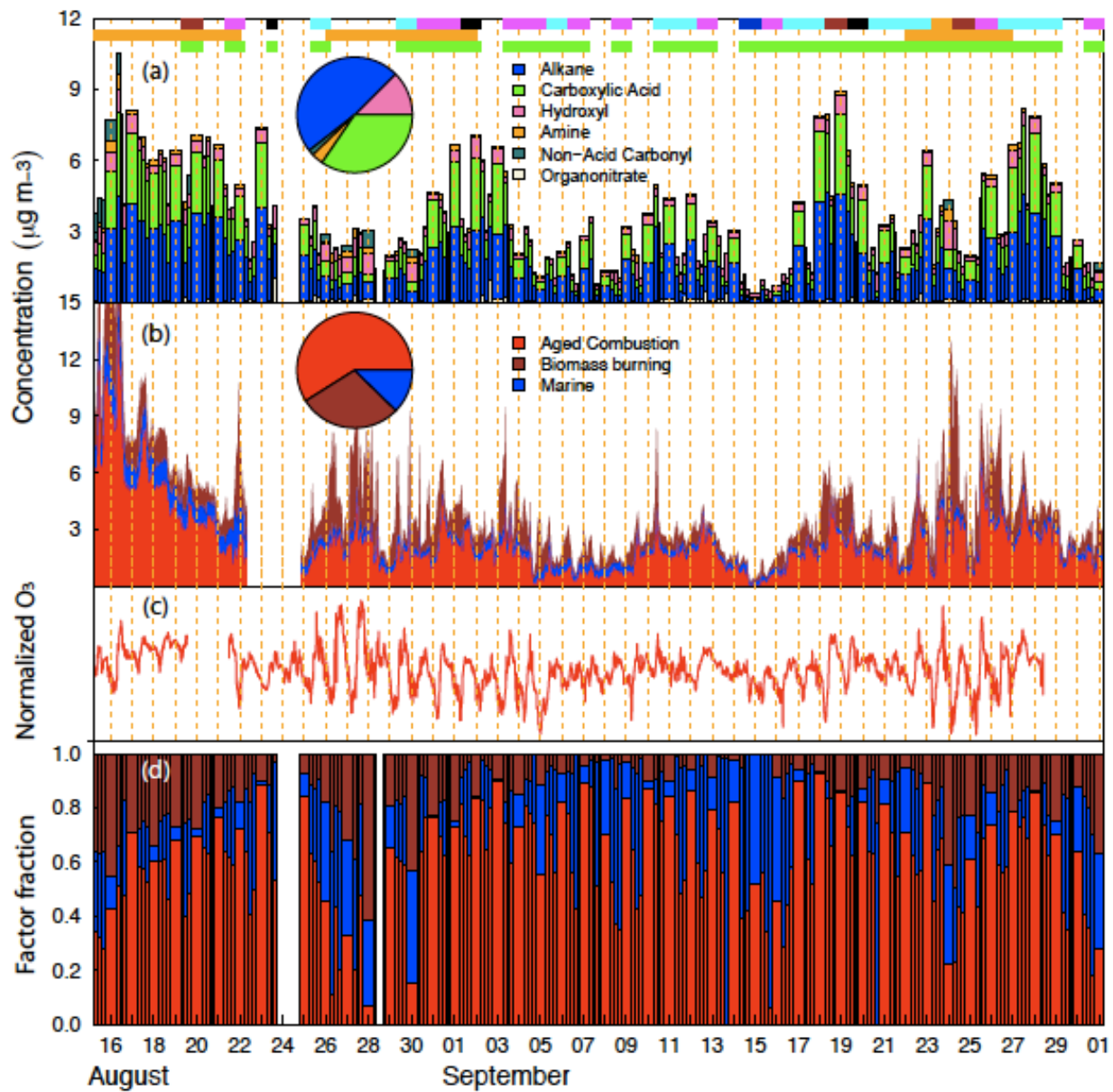


Fig. 3 (Fig. 2 in the revised manuscript): (a) Time series of organic functional group concentrations measured by the FTIR; sectors are indicated by the top color bars (same colors as in Fig. 1), for which the sector associated with each FTIR sample was determined as the air mass origin shown by the majority (>80%) of the back trajectories during the sampling time; top brown bars indicate fire periods corresponding to the La Brea fire (in Santa Barbara County), the Station fire (in Los Angeles County), and the Guiberson fire (in Ventura County), respectively (from left to right); top green bars indicate samples that were used for diurnal profile analysis. (b) Time series of AMS factors identified by PMF analysis. The inner pie charts in (a) and (b) respectively show campaign average compositions of FTIR components and AMS factors. (c) Time series of normalized  $\text{O}_3$  (normalized by campaign average) mixing ratio. (d) Mass fractions of the FTIR combustion factor (red), the biomass burning factor (brown), and the marine factor (blue) during the measurement.

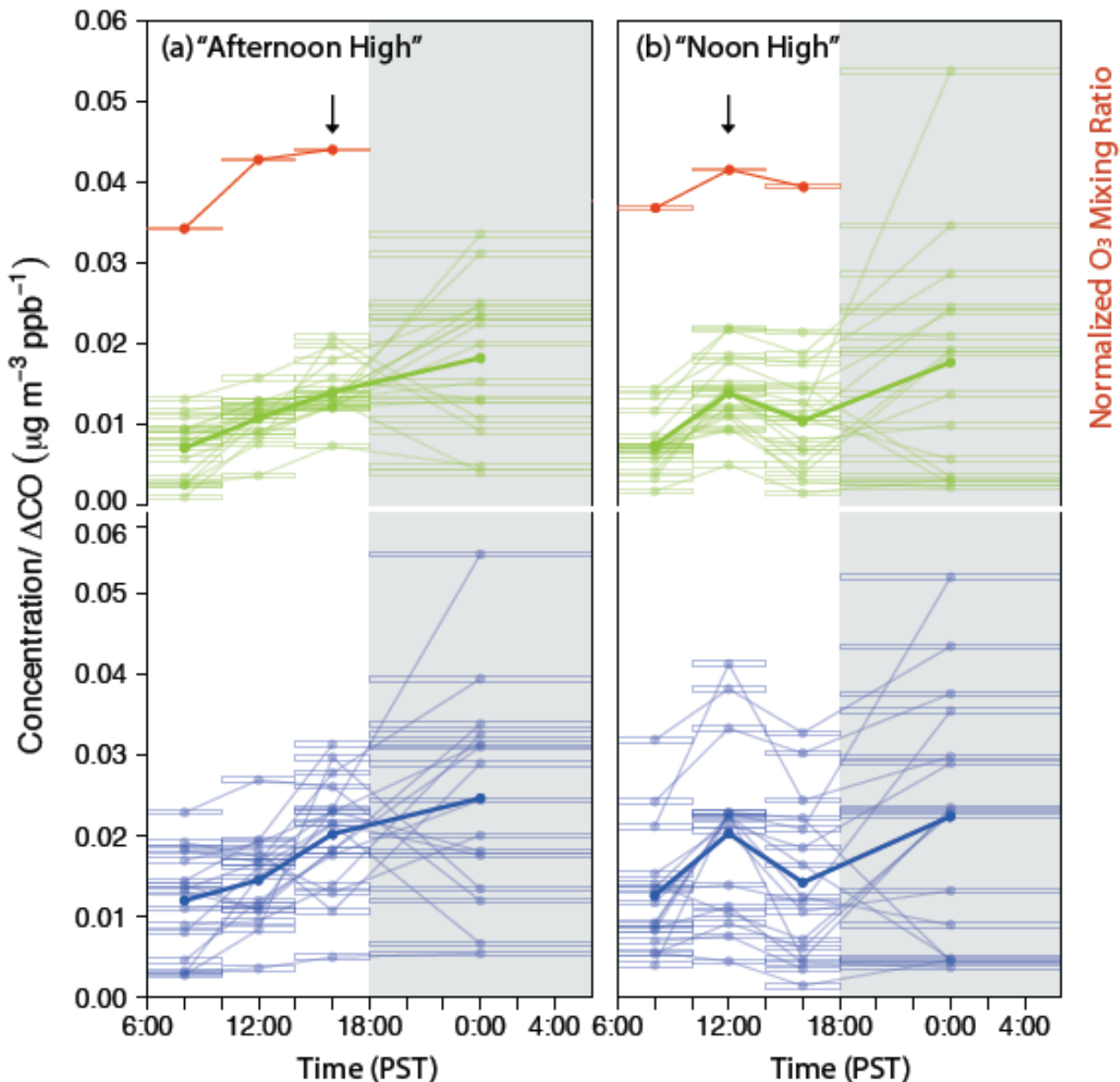


Fig. 6 (Fig. 4 in the revised manuscript): Diurnal cycles of normalized carboxylic acid group concentrations (green; top part in each panel) and alkane group concentrations (blue; bottom part in each panel) divided into (a) "Afternoon High" and (b) "Noon High" types. Each rectangle represents one FTIR sample with the length of the rectangle indicating the sampling duration. The lines connecting the rectangles show samples collected in the same day. The thinner rectangles and lines represent daily diurnal profiles, while the thicker lines show the averages for the days in the corresponding panel. The red dashed lines represent average diurnal profiles of normalized O<sub>3</sub> mixing ratio for the days in each panel. The arrows indicate daytime peak concentration in each panel. Shaded areas indicate nighttime periods corresponding to the FTIR nighttime samples, which were excluded from the diurnal cycle analyses.

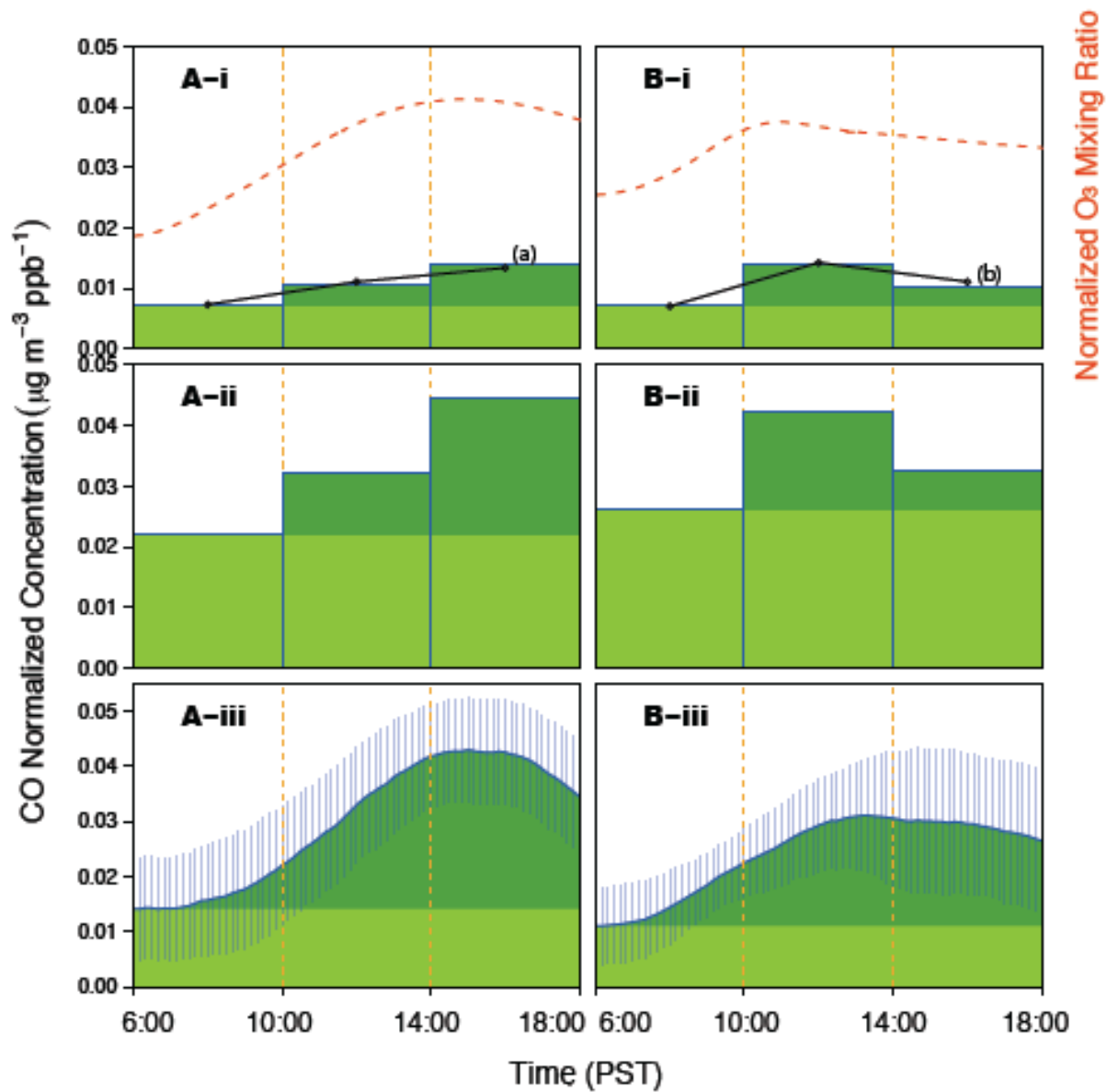


Fig. 12 (Fig. 10 in the revised manuscript): Daytime profiles of A (“Afternoon High” days) and B (“Noon High” days) for (i) carboxylic acid group, (ii) the FTIR combustion factor, and (iii) the AMS combustion factor concentration. Colors indicate “Background SOA” (light green) and “12-h daytime SOA” (dark green), respectively. Red dashed lines in panels A-i and B-i represent average daytime profiles of normalized O<sub>3</sub>. Black lines in panels A-i and B-i are the average diurnal carboxylic acid group profiles corresponding to the two panels shown in Fig. 4 as indicated by the labels beside the lines. Vertical blue bars in panels A-iii and B-iii show standard deviations of the averaged diurnal cycles.

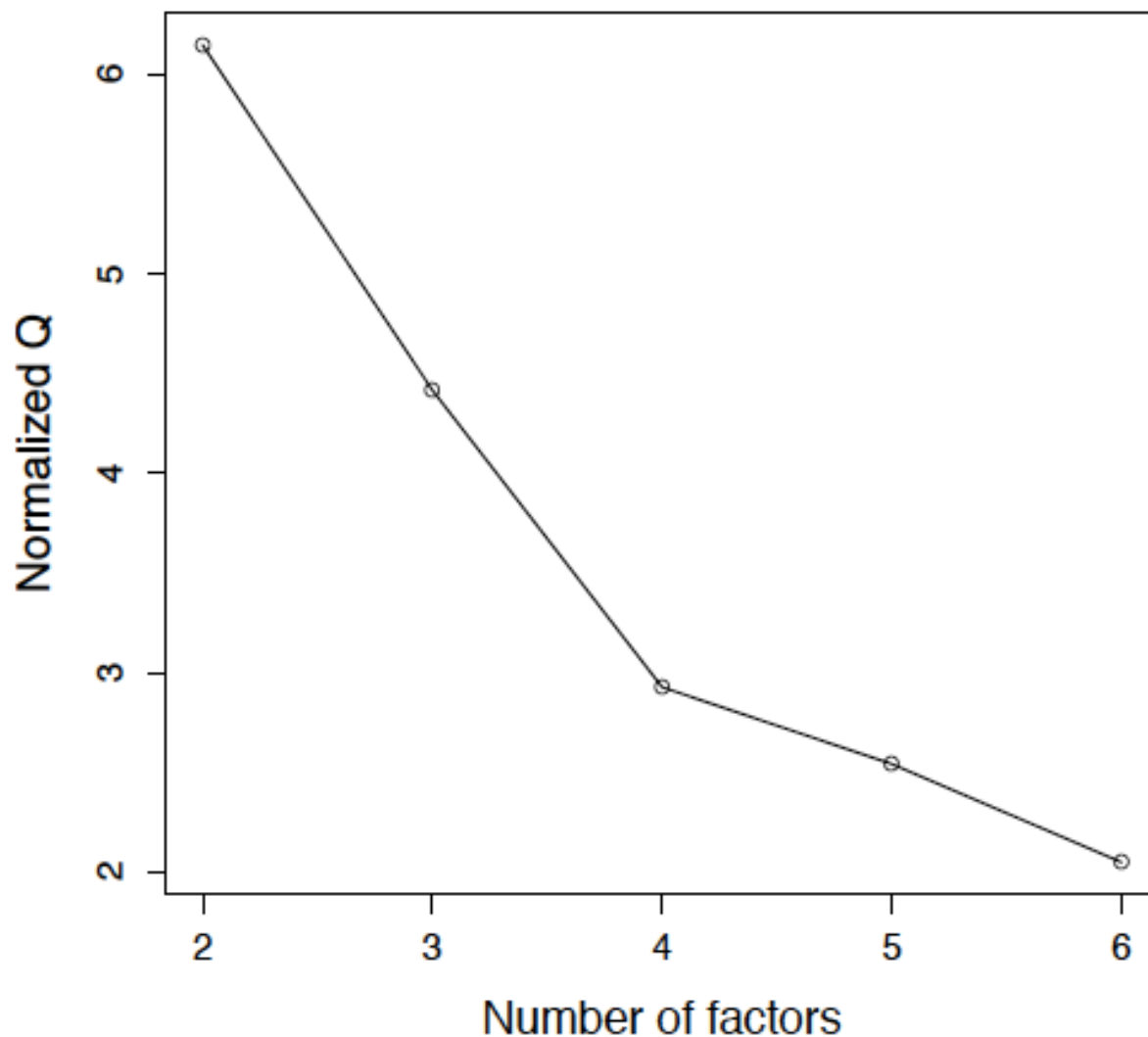


Fig. A1: Normalized Q values versus number of factors for the FTIR PMF analysis.

References (references in the manuscript are not shown here):

Claeys, M., Szmigielski, R., Kourtchev, I., Van der Veken, P., Vermeylen, R., Maenhaut, W., Jaoui, M., Kleindienst, T., Lewandowski, M., Offenberg, J., and Edney, E. O.: Hydroxydicarboxylic acids: Markers for secondary organic aerosol from the photooxidation of  $\alpha$ -pinene, *Environ. Sci. Technol.*, 41, 1628–1634, 2007.

Cronn, D.R., Charlson, R.J., Knights, R.L., Crittenden, A.L., and Appel, B.R.: A survey of the molecular nature of primary and secondary components of particles in urban air by high-resolution mass spectrometry, *Atmos. Environ.*, 11, 929–937, 1977.

DeCarlo, P. F., Ulbrich, I. M., Crouse, J., de Foy, B., Dunlea, E. J., Aiken, A. C., Knapp, D., Weinheimer, A. J., Campos, T., Wennberg, P. O., and Jimenez, J. L.: Investigation of the sources and processing of

organic aerosol over the Central Mexican Plateau from aircraft measurements during MILAGRO, *Atmos. Chem. Phys.*, 10, 5257–5280, 2010.

Dominguez, G., Jackson, T., Brothers, L., Barnett, B., Nguyen, B., and Thiemens, M.H.: Discovery and measurement of an isotopically distinct source of sulfate in Earth's atmosphere, *P. Natl. Acad. Sci.*, doi:10.1073/pnas.0805255105, 2008.

Gilardoni, S., Russell, L.M., Sorooshian, A., Flagan, R.C., Seinfeld, J.H., Bates, T.S., Quinn, P.K., Allan, J.D., Williams, B., Goldstein, A.H., Onasch, T. B., Worsnop, D. R.: Regional variation of organic functional groups in aerosol particles on four US east coast platforms during the International Consortium for Atmospheric Research on Transport and Transformation 2004 campaign, *J. Geophys. Res.-Atmos.*, doi:10.1029/2006JD007737, 2007.

Grosjean, D.: In situ organic aerosol formation during a smog episode: estimated production and chemical functionality, *Atmospheric Environment. Part A. General Topics*, 26, 953–963, 1992.

Hildebrandt, L., Engelhart, G.J., Mohr, C., Kostenidou, E., Lanz, V.A., Bougiatioti, A., DeCarlo, P.F., Prevot, A.S.H., Baltensperger, U., Mihalopoulos, N., Donahue, N. M., and Pandis, S. N.: Aged organic aerosol in the Eastern Mediterranean: the Finokalia aerosol measurement experiment-2008, *Atmos. Chem. Phys.*, 10, 4167–4186, 2010.

Kawamura, K. and Kaplan, I.R.: Motor exhaust emissions as a primary source for dicarboxylic acids in Los Angeles ambient air, *Environ. Sci. Technol.*, 21, 105–110, 1987.

Kawamura, K. and Ikushima, K.: Seasonal changes in the distribution of dicarboxylic acids in the urban atmosphere, *Environ. Sci. Technol.*, 27, 2227–2235, 1993.

Kawamura, K. and Yasui, O.: Diurnal changes in the distribution of dicarboxylic acids, ketocarboxylic acids and dicarbonyls in the urban Tokyo atmosphere, *Atmos. Environ.*, 39, 1945–1960, 2005.

Kleindienst, T.E., Conner, T.S., McIver, C.D., and Edney, E.O.: Determination of secondary organic aerosol products from the photooxidation of toluene and their implications in ambient PM 2.5, *Environ. Sci. Technol.*, 47, 79–100, 2004.

Liggio, J., Li, S.M., Vlasenko, A., Sjostedt, S., Chang, R., Shantz, N., Abbatt, J., Slowik, J.G., Bottenheim J.W., Brickell, P.C., Stroud, C., and Leitch, W.R.: Primary and secondary organic aerosols in urban air masses intercepted at a rural site, *J. Geophys. Res.-Atmos.*, 115, D21305, doi:10.1029/2010JD014426, 2010.

Lim, Y.B. and Ziemann, P.J.: Products and mechanism of secondary organic aerosol formation from reactions of n-alkanes with OH radicals in the presence of NO<sub>x</sub>, *Environ. Sci. Technol.*, 39, 9229–9236, 2005.

Lim, Y.B. and Ziemann, P.: Chemistry of secondary organic aerosol formation from OH radical-initiated reactions of linear, branched, and cyclic alkanes in the presence of NO<sub>x</sub>, *Aerosol. Sci. Tech.*, 43, 604–619, 2009.

Madronich, S., Chatfield, R.B., Calvert, J.G., Moortgat, G.K., Veyret, B., and Lesclaux, R.: A photochemical origin of acetic acid in the troposphere, *Geophysical Research Letters*, 17, 2361–2364, 1990.

Maria, S., Russell, L., Gilles, M., and Myneni, S.: Organic aerosol growth mechanisms and their climate forcing implications, *Science*, 306, 1921–1924, 2004.

Martin, P., Tuazon, E.C., Aschmann, S.M., Arey, J. and Atkinson, R.: Formation and atmospheric reactions of 4, 5-dihydro-2-methylfuran, *The Journal of Physical Chemistry A*, 106, 11492–11501, 2002.

Rogge, W.F., Hildemann, L.M., Mazurek, M.A., Cass, G.R., Simoneit, and B.R.T.: Sources of fine organic aerosol. 1. Charbroilers and meat cooking operations, *Environ. Sci. Technol*, 25, 1112–1125, 1991.

Rogge, W., Mazurek, M., Hildemann, L., Cass, G., and Simoneit, B.: Quantification of urban organic aerosols at a molecular level: identification, abundance and seasonal variation, *Atmos. Environ.*, 27, 1309–1330, 1993.

Russell, L.M, Bahadur, R. and Ziemann P.J.: Identifying organic aerosol sources by comparing functional group composition in chamber and atmospheric particles, *Proceedings of the National Academy of Sciences*, doi/10.1073/pnas.1006461108, 2011.

Satsumabayashi, H., Kurita, H., Yokouchi, Y., Ueda, H.: Mono-and di-carboxylic acids under long-range transport of air pollution in central Japan, *Tellus B*, 41, 219–229, 1989.

Satsumabayashi, H., Kurita, H., Yokouchi, Y., Ueda, H.: Photochemical formation of particulate dicarboxylic acids under long-range transport in central Japan, *Atmospheric Environment. Part A. General Topics*, 24, 1443–1450, 1990.

Sax, M., Zenobi, R., Baltensperger, U., and Kalberer, M.: Time resolved infrared spectroscopic analysis of aerosol formed by photo-oxidation of 1, 3, 5-trimethylbenzene and  $\alpha$ -pinene, *Aerosol. Sci. Tech.*, 39, 822–830, 2005.

Schuetzle, D., Cronn, D., Crittenden, A.L., and Charlson, R.J.: Molecular composition of secondary aerosol and its possible origin, *Environ. Sci. Technol*, 9, 838–845, 1975.

Ulbrich, I. M., Canagaratna, M. R., Zhang, Q., Worsnop, D. R., and Jimenez, J. L.: Interpretation of organic components from Positive Matrix Factorization of aerosol mass spectrometric data, *Atmos. Chem. Phys.*, 9, 2891–2918, 2009.

Zhang, Q., Jimenez, J.L., Canagaratna, M.R., Allan, J.D., Coe, H., Ulbrich, I., Alfarra, M.R., Takami, A., Middlebrook, A.M., Sun, Y.L., Dzepina, K., Dunlea, E., Docherty, K., DeCarlo, P. F., Salcedo, D., Onasch, T., Jayne, J. T., Miyoshi, T., Shimono, A., Hatakeyama, S., Takegawa, N., Kondo, Y., Schneider, J., Drewnick, F., Borrmann, S., Weimer, S., Demerjian, K., Williams, P., Bower, K., Bahreini, R., Cottrell, L., Griffin, R. J., Rautiainen, J., Sun, J. Y., Zhang, Y. M., and Worsnop, D. R.: Ubiquity and dominance of oxygenated species in organic aerosols in anthropogenically-influenced Northern Hemisphere midlatitudes, *Geophys. Res. Lett.*, 34, L13801, 2007b.